

Nanoscale

Accepted Manuscript



This is an *Accepted Manuscript*, which has been through the Royal Society of Chemistry peer review process and has been accepted for publication.

Accepted Manuscripts are published online shortly after acceptance, before technical editing, formatting and proof reading. Using this free service, authors can make their results available to the community, in citable form, before we publish the edited article. We will replace this *Accepted Manuscript* with the edited and formatted *Advance Article* as soon as it is available.

You can find more information about *Accepted Manuscripts* in the [Information for Authors](#).

Please note that technical editing may introduce minor changes to the text and/or graphics, which may alter content. The journal's standard [Terms & Conditions](#) and the [Ethical guidelines](#) still apply. In no event shall the Royal Society of Chemistry be held responsible for any errors or omissions in this *Accepted Manuscript* or any consequences arising from the use of any information it contains.

ARTICLE

Solution-processed assembly of ultrathin transparent conductive cellulose nanopaper embedding AgNWs

Cite this: DOI: 10.1039/x0xx00000x

Yuanyuan Song,^a Yaoquan Jiang,^b Liyi Shi,^b Shaomei Cao,^b Xin Feng,^{a,b,*} Miao Miao^b and Jianhui Fang^c

Received 00th January 2012,
Accepted 00th January 2012

DOI: 10.1039/x0xx00000x

www.rsc.org/

Natural biomass based cellulose nanopaper is becoming a promising transparent substrate to supersede traditional petroleum based polymer film in realizing future flexible paper-electronics. Here, ultrathin, highly transparent, outstanding conductive hybrid nanopaper with excellent mechanical flexibility was synthesized by the assembly of nanofibrillated cellulose (NFC) and silver nanowires (AgNWs) using a pressured extrusion paper-making technique. The hybrid nanopaper with thickness of 4.5 μm has a good combination of transparent conductive performance and mechanical stability using bamboo/hemp NFC and AgNWs cross-linked by hydroxypropylmethyl cellulose (HPMC). The heterogeneous fibrous structure of BNFC/HNFC/AgNWs endows uniform distribution and enhanced forward light scattering, resulting in highly electrical conductivity and optical transmittance. The hybrid nanopaper with an optimal weight ratio of BNFC/HNFC to AgNWs shows outstanding synergistic properties with transmittance of 86.41% at 550 nm and sheet resistance of 1.90 Ohm/sq, equal to the electronic conductivity, which is about 500 S/cm. The BNFC/HNFC/AgNWs hybrid nanopaper maintains a stable electrical conductivity after peeling test and bending at 135° for 1000 cycles, indicating remarkable strong adhesion and mechanical flexibility. Of importance here is that, the high-performance and low-cost hybrid nanopaper can offer a promising potential for electronics application in solar cell devices, flexible displays and other high-technology products.

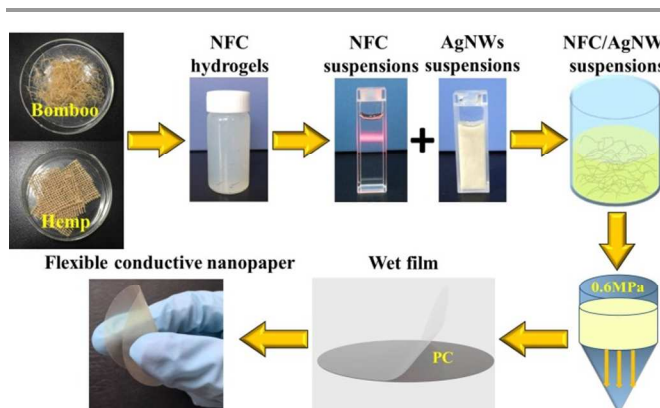
Introduction

Transparent conductive films fabricated on plastic substrates have received considerable attentions in recent years because of their simple processing and low manufacturing costs¹. However, the great challenge for transparent conductive plastic films is to sustain excellent mechanical durability and electrical continuity upon repeated bending or at high temperature processing². The device performance is strongly related to the improved tolerance for heat distortion and dimensional stability of plastics films during large temperature changes. Therefore, it is desirable to find a strong competitive replacement with excellent thermal stability that can be bent and even fully folded. Owing to its lightweight, flexibility, low thermal expansion, biodegradability, renewability, and enhanced printability, optical transparent nanopaper based on nanofibrillated cellulose (NFC) is emerging as an ideal platform to offer the potential to supersede petroleum-based polymers toward the future production of next-generation flexible and wearable electronics³⁻⁵. NFC nanopaper from abundant natural biomass is the suitable building block to house a range of guest

functional materials for flexible matrices with exciting synergistic properties⁶. Generally, indium tin oxide (ITO) has been widely used as transparent conductors due to its high transparency and low sheet resistance (over 80% and below 30 Ohm/sq) on a flexible substrate^{7,8}, but the inherent brittleness of ITO usually causes cracks upon bending or folding^{9,10}. To solve the problems, great efforts have been devoted to explore practical alternatives such as conducting polymers^{11,12}, graphene¹³⁻¹⁵, carbon nanotubes¹⁶⁻¹⁸, and metal nanowires^{19,20} for flexible transparent conductive films. Silver nanowires (AgNWs) are among the most promising candidates because of their exceptional transparency and high conductivity (95% and 20 Ohm/sq)²¹⁻²³. Considerable attention has been devoted to directly deposit conductive materials on the surface of flexible substrates using Mayer rod coating^{24,25}, wet coating²⁶⁻²⁸, and vacuum filtration²⁹⁻³¹. The significant challenge for the requirements of strong adhesion between conductive materials and transparent substrates need to be addressed³². In addition, pure AgNWs films can easily be oxidized to corrosion due to long time exposure in ambient air^{33,34}. Therefore, the development of hybrid transparent conductive films with high

performance by encapsulating AgNWs is becoming an important research issue³⁵. Chun et al. prepared a hybrid Ag-MWNT composite film with an average thickness of 140 μm by drop casting using a polyvinylidene fluoride (PVDF) copolymer as the matrix³⁶. Ghosh et al. developed a new transparent conductor comprising AgNWs embedded in an ultrathin polyimide (PI) foil that present a sheet resistance of 15 ohm/sq and very small thickness of 5 μm ³⁷. The transparent conductive performance is strongly related to the dispersion state of conductive nanomaterials and their conductive network integrity. NFC has been reported as an efficient dispersant for carbon nanotubes and 2D flakes³⁸⁻⁴⁰, and then provides the possibility to incorporate with conductive nanomaterials to construct uniformly heterogeneous interlaced network architectures. Transparent hybrid NFC nanopaper with multi-functional properties were prepared by a mimicking solution-based papermaking process, in which the aqueous NFC suspensions were dewatered through evaporation or vacuum filtration, followed by oven drying or hot pressing^{41,42}. In our previous work⁴³⁻⁴⁵, we developed a pressured-extrusion papermaking process to fast fabrication of luminescent NFC nanopaper with high transparency (over 90%). Highly oriented fibrous network combined with various functional guest materials were admirably achieved after quickly pressured dewatering process.

Herein, ultrathin, highly flexible, conductive and transparent bamboo/hemp NFC/AgNWs hybrid nanopaper 4.5 μm in thickness was successfully assembled using a solution-based pressured-extrusion paper-making process under 0.6 MPa of N_2 gas. The AgNWs were encapsulated under the surface of multiscale BNFC/HNFC fibrous network using HPMC as cross-linker. The ultrathin BNFC/HNFC/AgNWs nanopaper exhibited a sheet resistance of 1.90 ohm/sq with transmittance of 86.41% at 550 nm. Moreover, the strong adhesion and mechanical robustness of the hybrid nanopaper after peeling, bending and folding test were also investigated in detail. The outstanding synergistic properties of biomass based hybrid nanopaper combined with AgNWs will show great potential applications in versatile electronic devices, such as flexible displays, touch screens, solar cells and other devices.



Scheme 1 The schematic diagram of the solution-processed procedures of NFC/AgNWs nanopaper

Experimental

Materials

The sackcloth made from hemp fiber was collected from packaging industry and mechanical crushed to small fragment. Bamboo fiber was purchased from Fujian jianzhou bamboo development Co.,Ltd. Silver nanowires suspension (0.3wt%) with an average diameter of 50 nm and an average length of 20 ~30 μm was synthesized in our laboratory. Sodium hydroxide (NaOH), acetic acid (HAc) and sodium chlorite (NaClO_2) were purchased from Chemical reagent co., Ltd. Hydroxypropylmethyl cellulose I (HPMC) with viscosity of 4000 mPa.s was purchased from Aladdin Chemistry. All chemicals were of analytical grade and used without any further modification.

Preparation of NFC hydrogels

Hemp fiber and bamboo fiber were used as source material to prepare NFC suspensions. The procedure was shown as following. First, 10.0 g of the raw materials were pretreated and swelled with 3 wt% NaOH aqueous solution (300 g) at 80 $^\circ\text{C}$ for 4 h and filtered with deionized water until pH~7 to remove dissociative lignin and some pectin. Then, The cellulosic materials were bleached at 100 $^\circ\text{C}$ in 0.7 wt% NaClO_2 aqueous solution adjusted by HAc for 2 h with constant stirring, followed by filtrating and washing to neutral pH. After decoloration, the mixtures were centrifuged several times at 5000 r/min to remove excess liquid until reaching neutral pH, and subsequently ultrasonic smashed with a high frequency ultrasonic cell crusher (HighNova instrument Co, Ltd) at 1000 W for 0.5 h. Finally, hemp NFC (HNFC) and bamboo NFC (BNFC) hydrogels were successfully synthesized after further refined by a homogenization process with a high pressure homogenizer (D-3L, PhD Technology LLC, USA) for 3 cycles at a pressure of 172 MPa.

Preparation of NFC/AgNWs hybrid suspensions

HNFC hydrogels, BNFC hydrogels and HNFC/BNFC hybrid hydrogels were firstly ultrasonic dispersed in 100g deionized water for 15 min to form 0.5 wt% aqueous suspensions, respectively. Then, AgNWs suspension (0.3 wt%) was slowly added into NFC suspensions in a given ratio under magnetic stirring for 1 h. Finally, 0.3 g HPMC dissolved in distilled water (0.35 wt%) was introduced to the aforementioned suspension to obtain uniform blended dispersions, named as BNFC/AgNWs suspension, HNFC/AgNWs suspension and BNFC/HNFC/AgNWs suspension, respectively.

Fabrication of NFC/ AgNWs hybrid nanopaper

The as-prepared hybrid suspensions were poured into the extruder (NanoAble-150, PhD Technology LLC, USA) to remove excess water under 0.6 MPa of N_2 gas for 40 min using a nuclepore track-etch filter membrane (200 nm PC, Whatman, UK). After extrusion, the wet film was carefully peeled off from the PC filter membrane, sandwiched between two pieces

of glass sheets and then dried at 125 °C for 10 min. The NFC/AgNWs hybrid nanopapers with 45 mm in diameter were ultimately fabricated (hereinafter referred to as BNFC/AgNWs nanopaper, HNFC/AgNWs nanopaper and BNFC/HNFC/AgNWs nanopaper, respectively). The schematic diagram of the solution-processed procedures of NFC/AgNWs nanopaper is shown in Scheme 1.

Instruments and characterization

The morphologies of NFC and AgNWs were measured by transmission electron microscopy (TEM) (JEM-2010F, JEOL, Japan) operated at a 120 kV accelerating voltage. The surface morphologies of the as-prepared NFC/AgNWs nanopaper were observed using a field emission-scanning electron microscope (SEM) (S-4800, Hitach, Japan) and an atomic force microscopy (AFM) (Veeco Dimension 3100). The phase structures of NFC/AgNWs nanopaper were characterized by a powder X-ray diffraction (XRD) (D/max 2550, Rigaku, Japan) operating at 40 kV and 40 mA. Sheet resistance (R_s) of the NFC/AgNWs was tested using the standard four probe technique (RTS-8, China) and the measurements were averaged on 3 replicates. The optical transmittance of the hybrid film was carried out on a UV-Vis spectrophotometer (2501PC, SHIMADZU, Japan). The thermal stability of NFC/AgNWs nanopaper was studied by a thermogravimetric analyzer (TGA, STA409PC, Netzsch, Germany) at the heating rate of 10°C/min in the range of 30–900 °C under nitrogen atmosphere.

Results and discussion

The appearance of isolated NFC suspensions has a bright channel when shining a light with a laser beam (Scheme 1), that called “Tyndall effect”. It can be concluded that the colloidal suspensions are very stable and the size of NFC are all in nanometric. The morphologies are clearly discerned from the TEM images shown in Fig. 1 that the BNFC has a narrower size distribution than that of HNFC. The BNFC is mainly composed of nanofibers with 10–15 nm in diameter and 500–1000nm in length (Fig. 1a), while HNFC ranges from 20 nm to 50 nm in diameter and 1000–2000 nm in length (Fig. 1b). The results indicated that regular bamboo fiber and hemp fiber were successfully disintegrated into nanocrystalline cellulose with an average diameter of tens of nanometers and a length of hundreds of nanometers to several micrometers after chemical cleavage of amorphous non-cellulosic regions. As the fiber diameter is smaller than 50 nm, NFC will act as an excellent building block for developing transparent platform with tailored optical and mechanical properties⁴⁶. Fig. 1c displays TEM images of the BNFC/HNFC/AgNWs composites. Blended BNFC/HNFC is blurry in the image because of its smaller size and deficient crystallinity compared to AgNWs. The image shows that different sizes of BNFC/HNFC conjoin together to form a fibrous network structure. It is obvious that the well-dispersed AgNWs are closely combined with BNFC/HNFC fibrous network. The tangled fibrous network is beneficial to expand the pathway of AgNWs to make them fully contact for establishing electrical network.

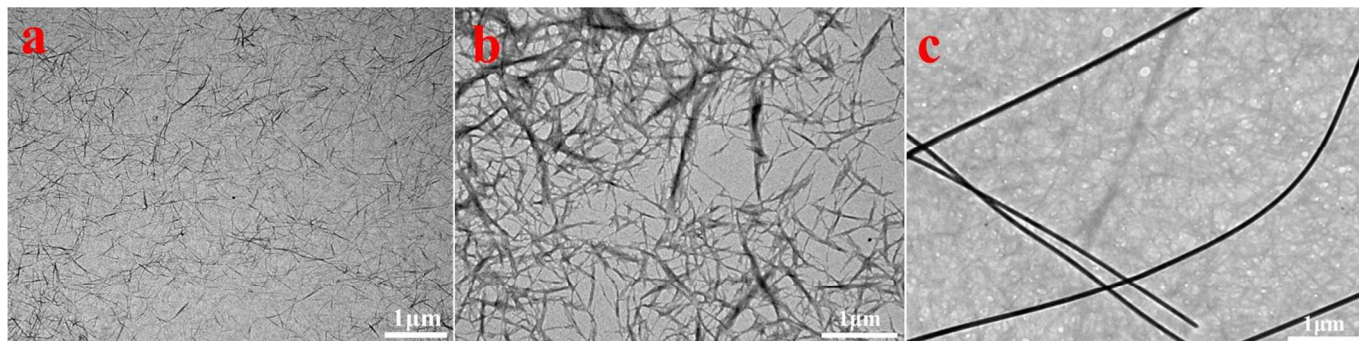


Fig.1 TEM images of (a) BNFC, (b) HNFC and (c) BNFC/HNFC/AgNWs.

Digital pictures of BNFC/HNFC/AgNWs hybrid nanopaper obtained by using the pressured-extrusion process are presented in Fig. 2. It is obvious that the hybrid nanopaper displays high optical transparency, indicating that AgNWs combined uniformly with BNFC/HNFC reduces light scattering of the hybrid nanopaper. However, the transmittance of the hybrid nanopaper decreases with the increasing of stoichiometric ratio of BNFC/HNFC to AgNWs from 1:0.4 to 1:1. The result is verified from that the school emblem of Shanghai University under the hybrid films which becomes more obscure. SEM and AFM images of the surface and fracture section of BNFC/HNFC/AgNWs hybrid nanopaper are presented in Fig. 3. It can be obviously observed from the top-view FE-SEM image

as shown in Fig. 3a that the AgNWs appears to be more uniformly distributed in the BNFC/HNFC substrate by intertwining with each other^{32,47}. Therefore, the closely packed electrical network structure was constructed after the pressured-extrusion to remove excess water. The fast dewatering process is an efficient paper-making method for well dispersed hybrid suspensions to fast fabricate a physically compact nanopaper with uniformly heterogeneous fibrous network architecture because of drainage in the perpendicular direction through the plenty of nanopores in paper matrix³². It can be clearly demonstrated that the AgNWs junctions are soldered by BNFC/HNFC using HPMC as the cross-linker (red cycles in Fig.3a). The knotted AgNWs junctions are beneficial to reduce

inter-nanowire contact resistance and greatly enhance the electrical conductivity^{48,49}. The long AgNWs renders a significant electrical network while still enabling high optical transparency for hybrid nanopaper. It can also be seen from AFM height image (Fig. 3b) that AgNWs are well dispersed in a NFC matrix. The AgNWs embedded under the surface of hybrid nanopaper without large surface roughness was clearly confirmed by 3D AFM image (see Supporting Information, Fig. S1). The fibrous nature of the nanopaper is further verified from the cross-sectional SEM images as shown in Fig. 3c,d, it can be observed that the well-stacked nanopaper with 4.5 μm in thickness represents poriferous fibrous structure combined with NFC and AgNWs blended fibers perpendicular to the breaking direction. It can be deduced that the nanofibrous bundles may be strongly linked together to display excellent mechanical properties for the BNFC/HNFC/AgNWs hybrid nanopaper.

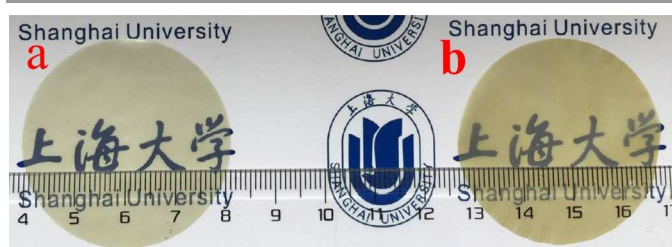


Fig.2 Digital pictures of BNFC/HNFC/AgNWs hybrid nanopaper with the weight ratio of BNFC/HNFC to AgNWs of (a) 1:0.4 and (b) 1:1.

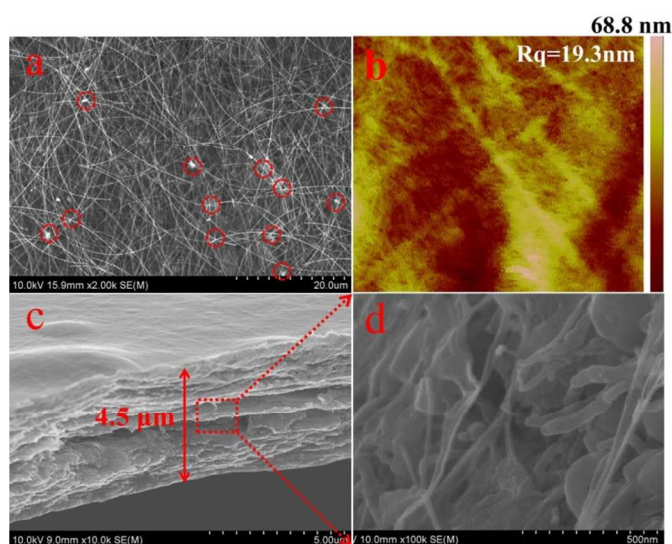


Fig.3 (a) Top-view FE-SEM image and (b) AFM image of the BNFC/HNFC/AgNWs hybrid nanopaper with a weight ratio of BNFC/HNFC to AgNWs of 1:1; (c,d) Cross-sectional SEM images of BNFC/HNFC/AgNWs hybrid nanopaper.

The phase structure and composition of hybrid nanopaper were further analysed by XRD measurement. As revealed in Fig. 4, the peaks at 16.4° and 22.4° can be indexed the typical (101) and (200) reflections of cellulose I. Except for characteristic peaks of NFC, all the other diffraction peaks at 38.12°, 44.32°, 65.54°, 77.40°, 81.53° are attributed to the diffraction of the (111), (200), (220), (311) and (222) crystal plane of the face-centered cubic silver (No. 04-0783), respectively. It is

convincing implied that the as-prepared hybrid nanopaper is composed of cellulose and silver composites.

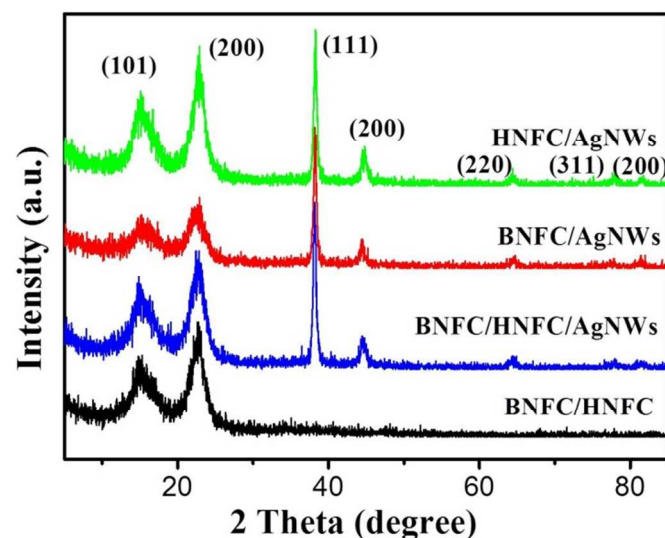


Fig.4 XRD patterns of BNFC/HNFC, BNFC/AgNWs, HNFC/AgNWs, and BNFC/HNFC/AgNWs hybrid nanopaper.

Fig. 5 shows the transparent conductive performances of HNFC/AgNWs and BNFC/HNFC/AgNWs hybrid nanopaper under the same conditions. And commercial ITO/PET conductive film is also evaluated as a reference. The ITO/PET film shows a sheet resistance of 11.50 ohm/sq and $T_{550\text{nm}}$ of 94.01%. It is obviously observed that BNFC/HNFC/AgNWs hybrid nanopaper displays much higher performance than /HNFC/AgNWs hybrid nanopaper with the same additive amount of AgNWs. The sheet resistance of BNFC/HNFC/AgNWs hybrid nanopaper (Fig. 1b) is 1.90 ohm/sq at wavelength of 550 nm, which is nearly 95 times lower than that of HNFC/AgNWs hybrid nanopaper. The difference perhaps comes from the different homogeneity of the electrical network. In a regular paper structure, all the fibers ranged into a random fibrous network with lots of air cavities⁵⁰. Therefore, careful attentions must be paid to how homogeneity is manipulated using different size of fibers to establish a uniformly heterogeneous multi-scale framework. So the ambition is to integrate AgNWs (50 nm in diameter), HNFC (20~50 nm in diameter) and BNFC (10~15 nm in diameter) together to construct strong interlaced BNFC/HNFC/AgNWs ternary system, where it is assumed that the cavities between larger HNFC and AgNWs was thoroughly filled by smaller BNFC and the connection was subsequently reinforced to form an interpenetrating electrical network.

BNFC/HNFC/AgNWs hybrid nanopaper comprised of various weight ratios of AgNWs (BNFC/HNFC to AgNWs; 1:1, 1:0.8, 1:0.6, 1:0.4) are demonstrated in Fig. 6. Each hybrid nanopaper has the equal amount of BNFC and HNFC. The larger size AgNWs added gradually increases light scattering and then decreases optical transparency. The transmittance of pure BNFC/HNFC nanopaper without AgNWs is 95% at a wavelength of 550 nm. It is evident that optical transmittance

increases with the decreasing of AgNWs concentration, as shown in Fig. 6a. For the BNFC/HNFC/AgNWs hybrid nanopaper with a weight ratio of 1:0.4, the optical transmittance reaches 93.63% (at 550 nm) with a sheet resistance of 24.63 ohm/sq. When the weight ratio of BNFC/HNFC to AgNWs is 1:1, the optical transmittance of the hybrid nanopaper decrease to 86.41% and the sheet resistance dramatically reduced to 1.90 ohm/sq, equal to the electronic conductivity, which is about 500 S/cm.

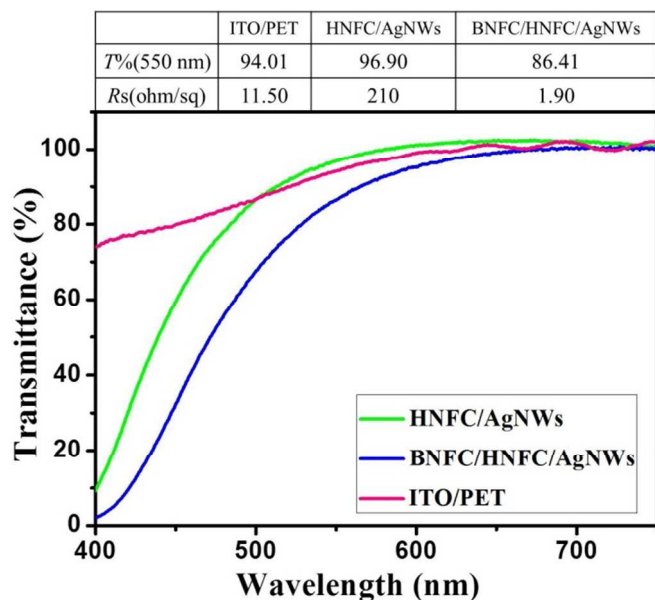


Fig.5 Transparent conductive performance of HNFC/AgNWs, BNFC/HNFC/AgNWs transparent paper and ITO/PET film.

The effect of drying temperature on the transparent conductive performances of BNFC/HNFC/AgNWs hybrid nanopaper was also investigated. Fig. 6b shows the optical transmittance and sheet resistance of BNFC/HNFC/AgNWs hybrid nanopaper at different drying temperature ranging from 100 to 200 °C. The hybrid nanopaper displays the best performances with the optical transmittance of 90.35% at a drying temperature of 125 °C. With the drying temperature rising constantly, the surface smoothness will be reduced due to the excessive thermal evaporation. The rough surface after higher drying temperature may contribute to enhancement of light scattering and decrease specular transmittance. Interestingly, the sheet resistances of all the hybrid nanopaper were little changed. Therefore, the outstanding performances are much better than those of ITO plastic films, indicating that the hybrid nanopaper with a proper amount of AgNWs providing an efficiently connected electrical network will meet the optoelectronic requirements for touch screen panel or solar cells. The initial degradation temperature is 300 °C that was much higher than conventional application temperature of conductive plastic film (see Supporting Information, Fig. S2). If a PET film is held at 150 °C for tens of minutes, the surface roughness will increase thus resulting in the decrease of optical transparency⁵¹.

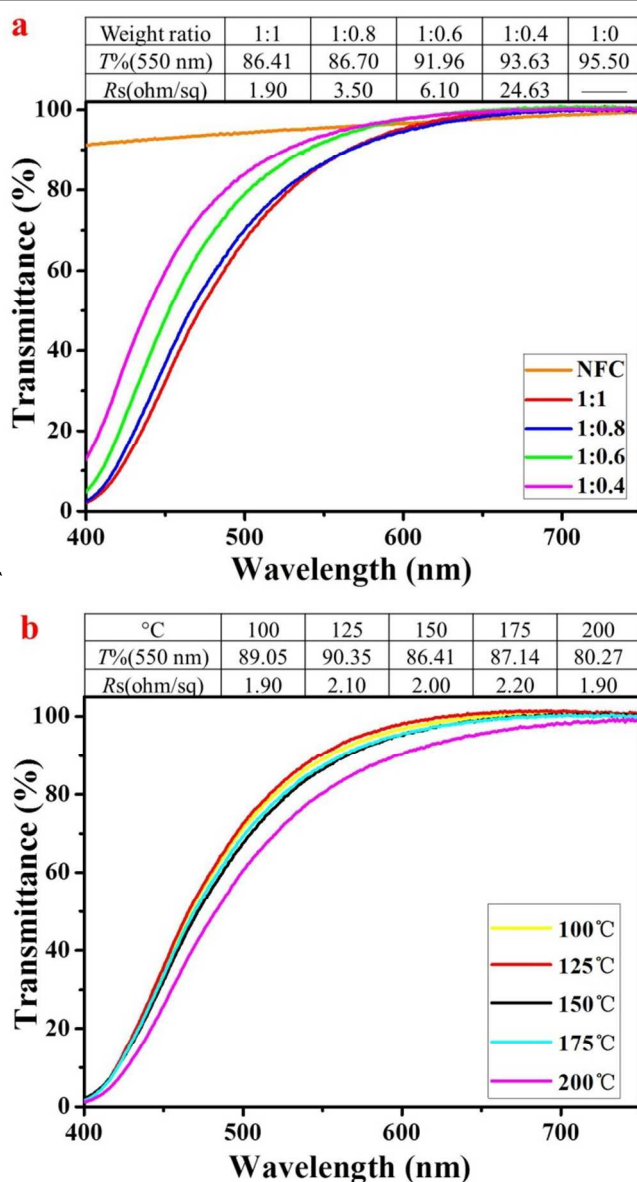


Fig.6 (a) Transparent conductive performance of BNFC/HNFC/AgNWs transparent paper with different AgNWs dosages; (b) Transparent conductive performance of BNFC/HNFC/AgNWs transparent paper with a weight ratio of BNFC/HNFC to AgNWs of 1:1 under different drying temperature.

Owing to the structural advantages and extraordinary electrical conductivity of ternary network system, BNFC/HNFC/AgNWs hybrid nanopaper exhibited excellent mechanical robustness against adhesion, friction and bending, which can be used a prospective candidate for flexible and stretchable conductors. Fig. 7a shows digital pictures of the hybrid nanopaper with a weight ratio of BNFC/HNFC to AgNWs is 1:1 using adhesive tape for peeling test. The performance of hybrid nanopaper with superior adhesion was maintained even after the peeling off test for 60 cycles (see Supporting Information, Fig. S3). In contrast, AgNWs deposited on PET film (Fig. 7b) was easily peeled off from the substrate^{7,8}. It can be noted that the intrinsically AgNWs fragile network anchored into BNFC/HNFC matrix becomes mechanically flexible, as shown in Fig. 7c. The

electrical resistance was negligibly changed after bending at 135° for 1000 cycles. Whereas the sheet resistance of commercial ITO/PET conductive film drastically increased by more than 10 times after the same bending cycles. In addition, the BNFC/HNFC/AgNWs hybrid nanopaper was successfully used to light a light-emitting diode (LED, 3V). It is obvious that the LEDs still give off bright light even after bending 1000 cycles (Fig. 7d,e). Moreover, the hybrid nanopaper exhibited an excellent morphological stability after folding, whereas the

commercial ITO/PET conductive film displayed lots of microscopic cracks along the direction perpendicular to that of folding stress due to the stiff ITO coating (see Supporting Information, Fig. S4). The results further confirm that the conductive hybrid nanopaper has excellent mechanical durability performance. Hence, it can be concluded that the AgNWs junctions embedded into BNFC/HNFC to form a stable multiscale heterogeneous electrical network with strong adhesion and outstanding mechanical flexibility.

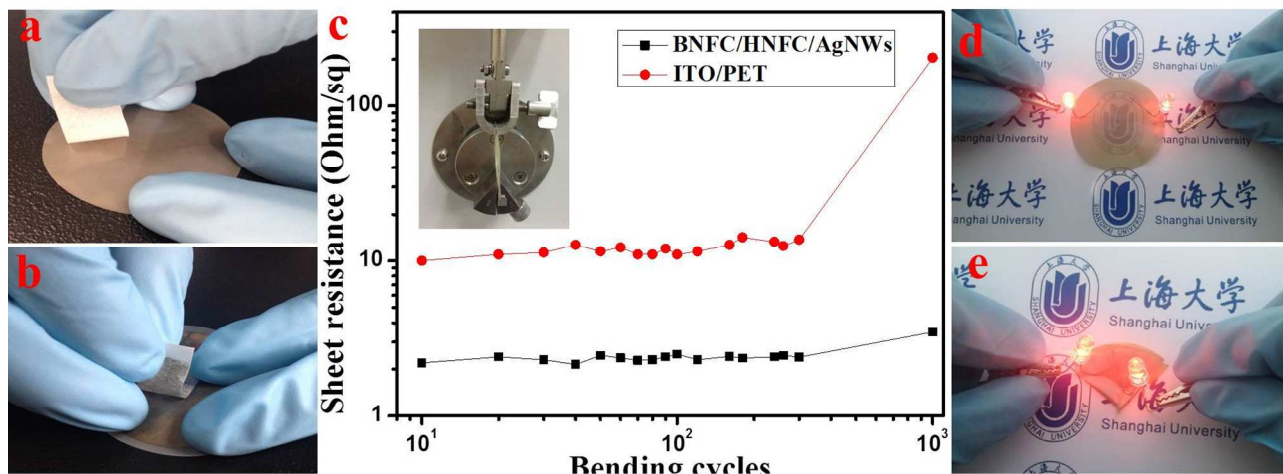


Fig. 7 Digital pictures of (a) BNFC/HNFC/AgNWs hybrid nanopaper and (b) AgNWs deposited on PET substrate after the peeling test; (c) Sheet resistance of BNFC/HNFC/AgNWs hybrid nanopaper and commercial ITO/PET film as a function of bending cycles, the inset shows image of the bending test machine used; (d) The lighting of two light-emitting diode (LED, 3V) placed between the BNFC/HNFC/AgNWs hybrid nanopaper (d) before and (e) after bending at 135° for 1000 cycles.

Conclusions

In summary, we have successfully fabricated an ultrathin, highly transparent conductive nanopaper using a solution-based pressured-extrusion aqueous paper-making process under 0.6 MPa of N₂ gas. The hybrid nanopaper was fast assembled with bamboo/hemp NFC as fibrous network, AgNWs as conductive fillers and HPMC as cross-linker. Thus AgNWs encapsulated into the BNFC/HNFC fibrous network and then the uniform multiscale heterogeneous electrical network architecture was ultimately established. The ultrathin BNFC/HNFC/AgNWs hybrid nanopaper 4.5 μm in thickness demonstrated excellent transparent conductive performance and strong mechanical durability. The hybrid nanopaper possesses high optical transmittance (86.41% at 550 nm), low sheet resistance (1.90 Ohm/sq), strong adhesion and mechanical flexibility, which can be used to fabricate efficient, flexible and printable paper electronic devices for future applications. On the basis of the solution-processed method and easily recyclability, cellulose based transparent nanopaper will offer an increasing potential for eco-friendly, portable and easily up-scalable devices production that outperform ITO/PET based devices.

Acknowledgements

This work was financially supported by the Science and Technology Commission of Shanghai Municipality

(13ZR1415100, 15ZR1415100, 13JC1402700). The authors are also grateful to Instrumental Analysis & Research Center of Shanghai University.

Notes and references

- ^a School of Materials Sciences and Engineering, Shanghai University, Shanghai 200444, P. R. China. Fax: 86-21-66136038; Tel: 86-21-66137257; E-mail: fengxin@shu.edu.cn
- ^b Research Center of Nano Science and Technology, Shanghai University, Shanghai 200444, P. R. China.
- ^c Department of Chemistry, Shanghai University, Shanghai 200444, P. R. China.
- M. Österberg, J. Vartiainen, J. Lucenius, U. Hippi, J. Seppälä, R. Serimaa and J. Laine, *ACS Appl. Mater. Interfaces*, 2013, **5**, 4640–4647.
 - B. D. Gates, *Science*, 2009, **323**, 1566–1567.
 - M. Henriksson, L. A. Berglund, P. Isaksson, T. Lindström and T. Nishino, *Biomacromolecules*, 2008, **9**, 1579–1585.
 - J. Kang, Y. Jang, Y. Kim, S. -H. Cho, J. Suhr, B.H. Hong, J. -B. Choi and D. Byun, *Nanoscale*, 2015, **7**, 6567–6573.
 - H. Sehaqui, Q. Zhou, O. Ikkala and L. A. Berglund, *Biomacromolecules*, 2011, **12**, 3638–3644.
 - H. L. Zhu, B. B. Narakathu, Z. Q. Fang, A. T. Aijazi, M. Joyce, M. Atashbar and L. B. Hu, *Nanoscale*, 2014, **6**, 9110–9115.
 - D. Lee, H. Lee, Y. Ahn and Y. Lee, *Carbon*, 2015, **81**, 439–446.
 - D. Paeng, J. -H. Yoo, J. Yeo, D. Lee, E. Kim, S. H. Ko and C. P. Grigoropoulos, *Adv. Mater.*, 2015, **27**, 2762–2767.

- 9 D. S. Hecht, L. Hu and G. Irvin, *Adv. Mater.*, 2011, **23**, 1482–1513.
- 10 H. Kang, S. Jung, S. Jeong, G. Kim and K. Lee, *Nat. Commun.*, 2015, **6**, 6503.
- 11 D. J. Lipomi, J. A. Lee, M. Vosgueritchian, B. C. K. Tee, J. A. Bolander, Z. Bao, *Chem. Mater.*, 2012, **24**, 373–382.
- 12 M. Vosgueritchian, D. J. Lipomi and Z. Bao, *Adv. Funct. Mater.*, 2012, **22**, 421–428.
- 13 K. S. Kim, Y. Zhao, H. Jang, S. Y. Lee, J. M. Kim, K. S. Kim, J. -H. Ahn, P. Kim, J. -Y. Choi and B. H. Hong, *Nature*, 2009, **457**, 706–710.
- 14 D. Lee, H. Lee, Y. Ahn and Y. Lee, *Carbon*, 2015, **81**, 439–446.
- 15 K. -Y. Shin and J. Jang, *Chem. Commun.*, 2014, **50**, 6645–6648.
- 16 Y. C. Jung, D. Shimamoto, H. Muramatsu, Y. A. Kim, T. Hayashi, M. Terrones and M. Endo, *Adv. Mater.*, 2008, **20**, 4509–4512.
- 17 H. W. Gu and T. M. Swager, *Adv. Mater.*, 2008, **20**, 4433–4437.
- 18 Z. C. Wu, Z. H. Chen, X. Du, J. M. Logan, J. Sippel, M. Nikolou, K. Kamaras, J. R. Reynolds, D. B. Tanner, A. F. Hebard and A. G. Rinzler, *Science*, 2004, **305**, 1273–1276.
- 19 S. SeobáLee, S. HwanáKo, *Nanoscale*, 2012, **4**, 6408–6414.
- 20 J. Lee, S. Connor, Y. Cui and P. Peumans, *Nano Lett.*, 2008, **8**, 689–692.
- 21 S. De, T. M. Higgins, P. E. Lyons, E. M. Doherty, P. N. Nirmalraj, W. J. Blau, J. J. Boland and J. N. Coleman, *ACS Nano*, 2009, **3**, 1767–1774.
- 22 L. B. Hu, H. S. Kim, J. -Y. Lee, P. Peumans and Y. Cui, *ACS Nano*, 2010, **4**, 2955–2963.
- 23 M. Song, D. S. You, K. Lim, S. Park, S. Jung, C. S. Kim, D. H. Kim, D. G. Kim, J. K. Kim and J. Park, *Adv. Funct. Mater.*, 2013, **23**, 4177–4184.
- 24 C. -H. Liu and X. Yu, *Nanoscale Res. Lett.*, 2011, **6**, 75.
- 25 S. J. Lee, Y. -H. Kim, J. K. Kim, H. Baik, J. H. Park, J. Lee, J. Nam, J. H. Park, T. -W. Lee, G. -R. Yi and J. H. Cho, *Nanoscale*, 2014, **6**, 11828–11834.
- 26 T. Tokuno, M. Nogi, M. Karakawa, J. Jiu, T. T. Nge, Y. Aso and K. Suganuma, *Nano Res.*, 2011, **4**, 1215–1222.
- 27 Y. Liu, X. L. Zhao, B. Cai, T. F. Pei, Y. H. Tong, Q. X. Tang and Y. C. Liu, *Nanoscale*, 2014, **6**, 1323–1328.
- 28 D. Y. Choi, H. W. Kang, H. J. Sung and S. S. Kim, *Nanoscale*, 2013, **5**, 977–983.
- 29 P. Lee, J. Ham, J. Lee, S. Hong, S. Han, Y. D. Suh, S. E. Lee, J. Yeo, S. S. Lee, D. Lee and S. H. Ko, *Adv. Funct. Mater.*, 2014, **24**, 5671–5678.
- 30 L. B. Hu, H. Wu, F. L. Mantia, Y. Yang and Y. Cui, *ACS Nano*, 2010, **4**, 5843–5848.
- 31 H. Koga, M. Nogi, N. Komoda, T. Nge, T. Sugahara and K. Suganuma, *NPG Asia Mater.*, 2014, **6**, e93.
- 32 J. Jiu, M. Nogi, T. Sugahara, T. Tokuno, T. Araki, N. Komoda, K. Suganuma, H. Uchida and K. Shinozaki, *J. Mater. Chem.*, 2012, **22**, 23561–23567.
- 33 J. Li, W. N. Zhang, Q. G. Li and B. J. Li, *Nanoscale*, 2015, **7**, 2889–2893.
- 34 Q. S. Xu, W. F. Shen, Q. J. Huang, Y. Yang, R. Q. Tan, K. Zhu, N. Dai and W. J. Song, *J. Mater. Chem. C*, 2014, **2**, 3750–3755.
- 35 C. Preston, Z. Q. Fang, J. Murray, H. L. Zhu, J. Q. Dai, J. N. Munday and L. B. Hu, *J. Mater. Chem. C*, 2014, **2**, 1248–1254.
- 36 K.-Y. Chun, Y. Oh, J. Rho, J.-H. Ahn, Y.-J. Kim, H. R. Choi and S. Baik, *Nat. Commun.*, 2010, **5**, 853–857.
- 37 D. S. Ghosh, T. L. Chen, V. Mkhitarian and V. Pruneri, *ACS Appl. Mater. Interfaces*, 2014, **6**, 20943–20948.
- 38 Z. Q. Fang, H. L. Zhu, Y. B. Yuan, D. Ha, S. Zhu, C. Preston, Q. X. Chen, Y. Y. Li, X. G. Han, S. Lee, G. Chen, T. Li, J. Munday, J. S. Huang and L. B. Hu, *Nano Lett.*, 2014, **14**, 765–773.
- 39 N. T. Cervin, L. Andersson, J. B. S. Ng, P. Olin, L. Bergström and L. Wågberg, *Biomacromolecules*, 2013, **14**, 503–511.
- 40 Y. Y. Li, H. L. Zhu, F. Shen, J. Y. Wan, S. Lacey, Z. Q. Fang, H. Q. Dai and L. B. Hu, *Nano Energy*, 2015, **13**, 346–354.
- 41 Z. Weng, Y. Su, D. -W. Wang, F. Li, J. Du and H. -M. Cheng, *Adv. Energy Mater.*, 2011, **1**, 917–922.
- 42 H. Sehaqui, A. Liu, Q. Zhou and L. A. Berglund, *Biomacromolecules*, 2010, **11**, 2195–2198.
- 43 M. Miao, J. P. Zhao, X. Feng, Y. Cao, S. M. Cao, Y. F. Zhao, X. Q. Ge, L. N. Sun, L. Y. Shi and J. H. Fang, *J. Mater. Chem. C*, 2015, **3**, 2511–2517.
- 44 J. P. Zhao, Z. W. Wei, X. Feng, M. Miao, L. N. Sun, S. M. Cao, L. Y. Shi and J. H. Fang, *ACS Appl. Mater. Interfaces*, 2014, **6**, 14945–14951.
- 45 S. M. Cao, Y. Y. Song, X. Feng, H. J. Liu, M. Miao, J. H. Fang and L. Y. Shi, *ACS Appl. Mater. Interfaces*, 2015, **7**, 10695–10701.
- 46 H. L. Zhu, S. Parvinian, C. Preston, O. Vaaland, Z. C. Ruan and L. B. Hu, *Nanoscale*, 2013, **5**, 3787–3792.
- 47 X. Y. Zeng, Q. K. Zhang, R. M. Yu and C. Z. Lu, *Adv. Mater.*, 2010, **22**, 4484–4488.
- 48 J. Liang, L. Li, K. Tong, Z. Ren, W. Hu, X. Niu, Y. Chen and Q. Pei, *ACS Nano*, 2014, **8**, 1590–1600.
- 49 J. Lee, P. Lee, H. B. Lee, S. Hong, I. Lee, J. Yeo, S. S. Lee, T. -S. Kim, D. Lee and S. H. Ko, *Adv. Funct. Mater.*, 2013, **23**, 4171–4176.
- 50 Z. Q. Fang, H. L. Zhu, C. Preston, X. G. Han, Y. Y. Li, S. Lee, X. S. Chai, G. Chen and L. B. Hu, *J. Mater. Chem. C*, 2013, **1**, 6191–6197.
- 51 M. Nogi, C. Kim, T. Sugahara, T. Inui, T. Takahashi and K. Suganuma, *Appl. Phys. Lett.*, 2013, **102**, 181911.